

# Tetraiodophenolsulfonphthalein as a spectral substitute to characterize the complexation between cationic and anionic surfactant

Hong-Wen Gao<sup>a,\*</sup>, Yan Qian<sup>b</sup>, Zhang-Jun Hu<sup>c</sup>

<sup>a</sup> Key Laboratory of Changjiang River Water Environment of Ministry of Education, College of Environmental Science and Engineering, Tongji University, Shanghai 200092, People's Republic of China

<sup>b</sup> Institute of Chemistry, Chinese Academy of Sciences, Beijing 100080, People's Republic of China

<sup>c</sup> School of Chemistry and Chemical Engineering, Anhui University, Hefei 230039, People's Republic of China

Received 15 October 2003; accepted 17 June 2004

Available online 24 July 2004

## Abstract

The complexation of cetyltrimethylammonium bromide (CTAB) with sodium dodecyl sulfate (SDS) with sodium dodecyl benzene sulfonate (SDBS), with tetraiodophenolsulfonphthalein (TIPST) as a spectral substitute was investigated at pH 5.89 and 8.30 by the microsurface adsorption—spectral correction (MSASC) technique. The aggregations of TIPST, SDS, and SDBS on CTAB obeyed the Langmuir isothermal adsorption. The aggregates TIPST–CTAB, TIPST<sub>2</sub>–CTAB<sub>3</sub>, SDS<sub>3</sub>–CTAB<sub>2</sub>, and SDBS<sub>3</sub>–CTAB<sub>2</sub> were formed at 20 °C and the binding constants of all the aggregates were determined. The replacement of TIPST-binding CTAB monomer with SDS or SDBS at pH 5.89 was applied to the quantitative determination of anionic detergent (AD) in water with satisfactory recovery.

© 2004 Elsevier Inc. All rights reserved.

**Keywords:** MSASC technique; Tetraiodophenolsulfonphthalein; Surfactant–surfactant interaction; Langmuir aggregation; Determination of anionic detergent

## 1. Introduction

Surfactants are extensively applied to industrial production, mining, equipment and device washing, daily life, environmental protection, medical treatment and sanitation, and other aspects. Besides, they are often used in scientific research and academic laboratories, e.g., chemical separation, trace extraction, and organic synthesis, because of their solubilization and sensibilization functions. With respect to the surfactant's interaction with organic compounds and dyes [1–5], polymers [6–9], and biomacromolecules [10–12], many earlier investigations were reported in detail, which included the effect of size and valency of the counterion, electrolyte concentration, temperature, and addition of an anionic surfactant [13,14]. However, the studies in this area are still important and interesting for the theory and technology of dyeing, washing, separating, and sensibiliz-

ing. Investigations into the behavior of different substances in surfactant aqueous solutions can, among other things, give useful information about the mechanisms according to which surfactants operate as leveling agents and information on the influence of compound–surfactant interactions on the thermodynamics and kinetics of those processes. Experimental methods mostly used were spectroscopy, tensiometry, conductometry, extraction [15], and potentiometry [16,17]. Some earlier models were proposed to explain the synergism mechanism, e.g., synergism perturbation [18], hydrogen-bond formation [19], micelle catalysis [20], and rigid asymmetric microenvironments [21]. Each can explain certain specific appearances but is suitable either for only ionic surfactants or for only nonionic surfactant. We have established a novel approach named the MSASC technique to characterize the dye–ionic surfactant interaction [22,23], which is based on the Langmuir isothermal adsorption theory. In spite of the fact that the surfactant mixtures as leveling agents are of great practical importance because of their synergistic behavior, investigations into intermolecular inter-

\* Corresponding author. Fax: +86-21-6598-8598.

E-mail address: [hwgao@mail.tongji.edu.cn](mailto:hwgao@mail.tongji.edu.cn) (H.-W. Gao).

actions between organic compounds or dyes and surfactants in mixed surfactant systems are rare [24]. Because of the weak electrostatic connection between the hydrophilic group of the ionic surfactant and the counterion, ordinary spectroscopy, e.g., the UV method, is unfit for the direct measurement of surfactant–surfactant interaction. A spectral probe, e.g., dye, was once used as a substitute to investigate the interaction of surfactant with proteins [25]. We tried to select a proper ionic dye as substitute to determine the physicochemical properties of a cationic surfactant–anionic surfactant mixed solution. The aim was to find a suitable experimental method, a procedure, and an appropriate theoretical model for the quantitative study of surfactant–surfactant interactions. In this work, tetraiodophenolsulfonphthalein (TIPST) was chosen to characterize the interaction of cetyltrimethylammonium bromide (CTAB) with sodium dodecyl sulfate (SDS) and sodium dodecyl benzene sulfonate (SDBS). The structure of TIPST is given in Fig. 1. It forms anion at pH 5.89 and 8.30 and can be adsorbed on CTAB to form the CTAB–TIPST aggregate. The dye has a strong light-absorptivity at long wavelengths in neutral medium and the spectral shift of the aggregate is 60 nm at pH 5.89 and 15 nm

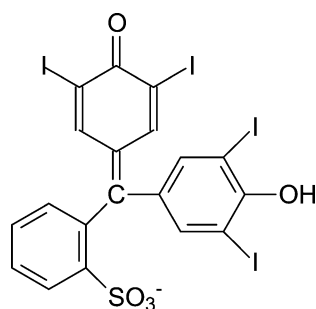


Fig. 1. Structure draw of TIPST.

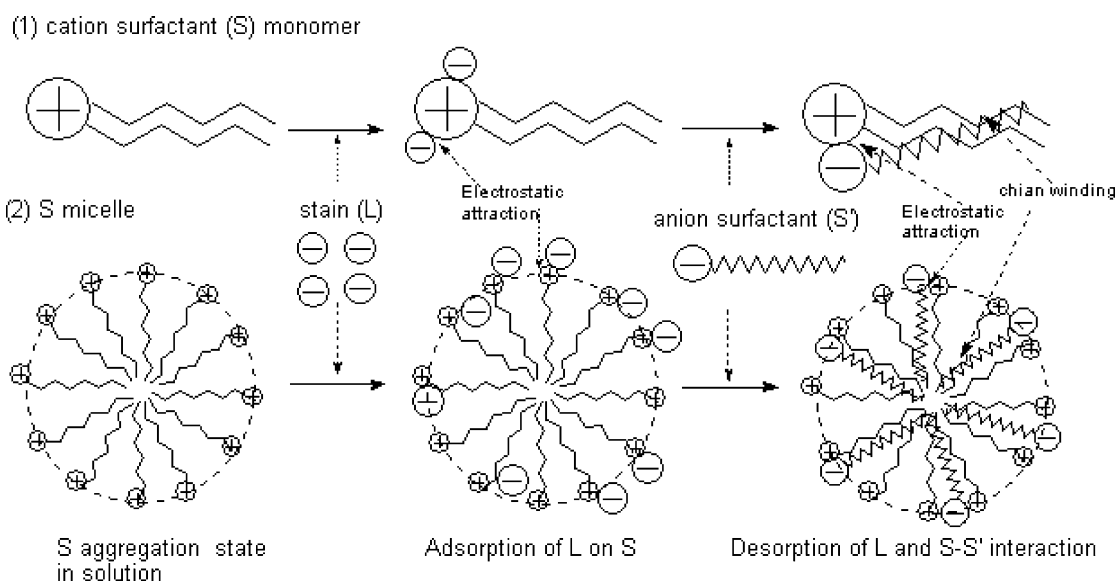


Fig. 2. Sketch for the aggregation of dye (L) on cationic surfactant (S) and interaction of S and anionic surfactant (S'). (Left, S ion state; Middle, aggregation of L on S; Right, desorption and replacement of L and aggregation of S' on S.)

at pH 8.30. Thus, spectrophotometry can be used in this work. In the CTAB–TIPST solution, the addition of an anionic surfactant (S'), SDS or SDBS, to substitute for the TIPST binding on CTAB was observed. The present work was done in the diluted surfactant's aqueous solutions so the surfactant was always in monomer form but not in micellar form. A novel method was developed for the investigation of the surfactant–surfactant interaction.

## 2. Principle

In Fig. 2, in surfactant (S), e.g., CTAB aqueous solution, the self-aggregation of S molecules forms a big electrostatic global micelle (Fig. 2, left) when S is above the critical micellar concentration (CMC). The electrostatic attraction of an oppositely charged dye (L) occurs on S monomers and micelles until kinetic equilibrium (Fig. 2, middle). The aggregation of L on S is in only a monolayer [22], so it obeys Langmuir isothermal adsorption [26]. The following equilibrium occurs in the L–S solution:

	L	+	S (m.s.)	→	SL <sub>n</sub> (m.s.)
Initial state	C <sub>L0</sub> (A <sub>0</sub> , A' <sub>0</sub> )		C <sub>S0</sub>		0
Equilibrium	C <sub>L</sub>				C <sub>S0</sub> (A <sub>c</sub> )

The Langmuir isothermal equation was used,

$$\frac{1}{\gamma} = \frac{1}{N} + \frac{1}{KNC_L}, \quad (1)$$

where  $K$  is the equilibrium constant and  $C_L$  the molarity of free L in the equilibrium solution. The symbol  $\gamma$  indicates the molar ratio of L adsorbed to S. With increased L concentration,  $\gamma$  approaches a maximum,  $N$ , called the

binding ratio. From the line for  $\gamma^{-1}$  vs  $C_L^{-1}$ , we may calculate  $N$  and  $K$ . Because the electrostatic connection is always weaker than a covalent bond, the spectral shift is often small in spite of the visible light range. The spectral correction technique must be used in place of ordinary spectroscopy. Therefore, both  $C_L$  and  $\gamma$  in Eq. (1) are calculated by means of [23]

$$\gamma = \eta \times \frac{C_{L_0}}{C_S}, \quad (2)$$

$$C_L = (1 - \eta)C_{L_0}, \quad (3)$$

where

$$\eta = \frac{A_c - \Delta A}{A_0}. \quad (4)$$

$C_S$  and  $C_{L_0}$  are the molarities of S and L added initially and  $\eta$  indicates the effective fraction of L.  $A_c$ ,  $A_0$ , and  $\Delta A$  are the real absorbance of the S–L product, the absorbance of the reagent blank against water and that of the S–L solution against the reagent blank, respectively, directly measured at the peak wavelength  $\lambda_2$ . The  $A_c$  is calculated by the relation [27],

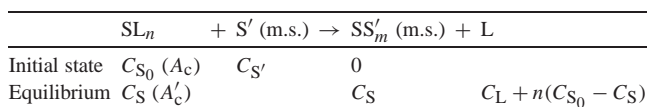
$$A_c = \frac{\Delta A - \beta \Delta A'}{1 - \alpha\beta}, \quad (5)$$

where  $\Delta A'$  indicates the absorbance of the S–L solution measured at the valley absorption wavelength  $\lambda_1$ . In common, both  $\alpha$  and  $\beta$  are the correction constants and they are determined by measuring  $SL_n$  and L solutions directly [23]. In addition, the molar absorptivity ( $\varepsilon_r^{\lambda_2}$ ) (it is not the apparent absorptivity,  $\varepsilon_a^{\lambda_2}$ ) of  $SL_n$  at  $\lambda_2$  is calculated by means of

$$\varepsilon_r^{\lambda_2} = \frac{NA_c}{\delta\gamma C_S}, \quad (6)$$

where  $\delta$  is the cell thickness (cm).

In the S–L solution, the addition of anionic surfactant ( $S'$ ) can substitute the L from its S aggregate as shown in Fig. 2, right. The replacement reaction is followed:



The calculation formulas are further delivered as follows [25]:

$$\gamma = m = \frac{C_{S_0} - C_S}{C_{S'}} = \frac{C_{S_0} - C_S}{C_{S_0}} \times \frac{C_{S_0}}{C_{S'}} = \eta \times \frac{C_{S_0}}{C_{S'}}, \quad (7)$$

$$C_S = C_{SL} = (1 - \eta)C_{C_{S_0}}, \quad (8)$$

where

$$\eta = \frac{A_c - A'_c}{A_c} = \frac{\Delta A_c}{A_c}. \quad (9)$$

The binding between S and  $S'$  involves the electrostatic attraction and their carbon chains' winding, so the interaction of  $S'$  with S is stronger than that of L with S. The

characterization of the S– $S'$  aggregate can be carried out by Eqs. (7), (8), and (9).

### 3. Experimental

#### 3.1. Materials and instruments

Absorption spectra were recorded on a Lambda 25 spectrophotometer (Perkin–Elmer Instruments, USA) with a 1-cm cell. The Model DDS-11A conductivity meter (Tianjin Sec. Anal. Instruments, China) was used to measure conductivity together with a Model DJS-1 conductivity immersion electrode (electrode constant 0.98, Shanghai Tienkuang Devices, China) in production of deionized water between 0.5 and 1 ( $\mu\Omega\text{ cm}$ )<sup>-1</sup>. The pH of the solution was measured with a 320-S pH meter (Mettler–Toledo Instruments, Shanghai, China). The temperature was adjusted and remained constant in electric heated thermostat bath, Model 116R (Changjiang Test Instruments, Tongzhou, China). A DSA 10 MK 2 Drop Shape Analysis System (Germany) was used to measure the surface tension of solutions.

#### 3.2. Preparations

A stock standard solution of CTAB (10.00 mmol/l) was prepared by dissolving cetyltrimethylammonium bromide (CTAB) (Shanghai Chemical Reagents) in deionized water at 30 °C and then 1.00 mmol/l CTAB was prepared daily by diluting the stock solution. The following anionic surfactant solutions were prepared to substitute TIPST from its CTAB aggregate: Both of stock SDS and SDBS solutions, 10.0 mmol/l were prepared by dissolving SDS and SDBS (Shanghai Chemical Reagents) in deionized water. They must be diluted before use. SDS was still used as the standard substance for detection of AD. The stock TIPST solution was prepared by dissolving 1.000 g of tetraiodophenolsulfonphthalein (TIPST, FW 857.97, dye content 95%, B.D.H. Laboratory Chemicals, British Drug Houses) in 50 ml of *N,N'*-dimethylformamide (DMF, A.R., Wulian Chemicals, Shanghai) and then diluting to 1000 ml with deionized water, which contains 1.107 mmol/l TIPST. In the characterization of the CTAB–TIPST aggregate, 0.2214 mmol/l TIPST was prepared daily by diluting the stock solution. The ammonia and acetic buffer solutions (pH 4.10–9.56) were used to adjust the acidity of solutions. A solution was prepared by mixing 20.0 ml of 1.107 mmol/l TIPST, 2.22 ml of 10.0 mmol/l CTAB, and 10 ml of pH 5.89 buffer solution and diluting to 100 ml with deionized water and it contains 0.200 mmol/l CTAB–TIPST aggregate without free CTAB. It was used in the desorption of TIPST from the aggregate and the interaction of CTAB with SDS and SDBS. To adjust the ionic strength of the aqueous solutions, 2 mol/l NaCl was used. A Na<sub>2</sub>EDTA solution (5%) was prepared to mask the foreign metal ions possibly coexisted

in samples. All reagents were of analytical grade and used without further purification.

### 3.3. Methods

For the aggregation of TIPST on CTAB, into a 25-ml calibrated flask were added an appropriate working solution of CTAB, 2.5 ml of buffer solution, and a known volume of 0.2214 mmol/l TIPST. The mixture was diluted to 25 ml with deionized water and mixed thoroughly. After 5 min, measured the absorbance of the solution at pH 5.89 at 630 and 590.5 nm and those at pH 8.30 at 576 and 614 nm, respectively, against the reagent blank treated in the same way without CTAB. All  $A_c$ ,  $\eta$ ,  $C_L$ , and  $\gamma$  of each solution were calculated.

For the determination of AD, 10.0 ml of a sample was taken in a 25-ml flask and 2.5 ml of pH 5.89 buffer solution, 2 ml of 5% Na<sub>2</sub>EDTA, and 1.0 ml of the CTAB–TIPST

aggregate solution were added. It was diluted to 25 ml and mixed well. After 5 min, the absorbances were measured at 630 and 590.5 nm against a reagent blank.  $A_c$  and  $\Delta A_c$  between the blank without AD and the sample solution were calculated.

## 4. Results and discussion

### 4.1. Effect of pH on spectra and spectral analysis

The absorption spectra of the CTAB–TIPST solutions at various pHs are shown in Fig. 3A. From spectra 1–14 and curves 15 and 16, we observe that the interaction occurs in a wide pH scope between 4.10 and 9.56. This is attributed to the fact that TIPST is univalent. By comparing the peak and valley of the spectra, it is more sensitive between pH 5.05 and 9.07. The formation of TIPST anion becomes dif-

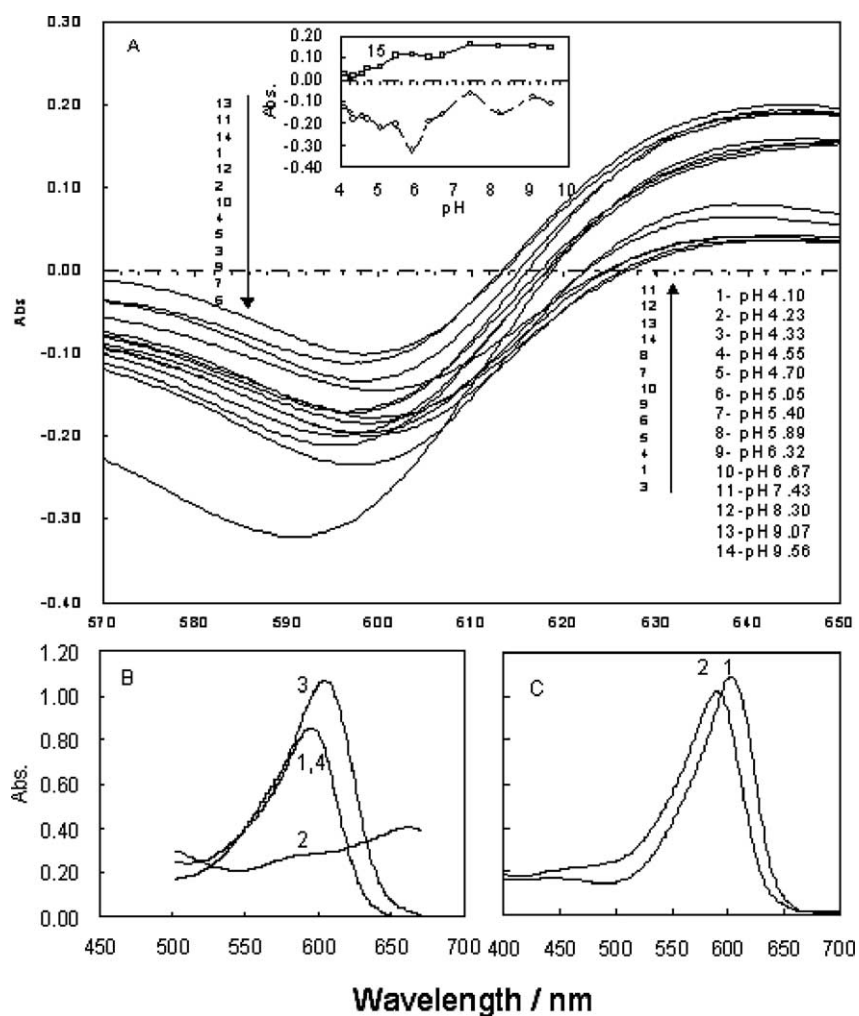


Fig. 3. (A) Effect of pH on the absorption spectra of the TIPST–CTAB solutions against reagent blank without CTAB: curves from 1 to 14 indicate pH from 4.10 to 9.56, where all the solutions contain 0.080 mmol/l CTAB and 0.02214 mmol/l TIPST. 15, absorbance variation at 630 nm; 16, same as 15 but at 590.5 nm. (B) Spectra of TIPST and its CTAB aggregate solution against water at pH 5.89: 1, 0.02214 mmol/l TIPST, 2, TIPST (0.02214 mmol/l)–CTAB (0.030 mmol/l) monomer aggregate, 3, TIPST (0.02214 mmol/l)–CTAB (1.00 mmol/l) micellar aggregate containing 0.02214 mmol/l TIPST, and 4, TIPST (0.02214 mmol/l)–CTAB (0.030 mmol/l)–SDS (1.00 mmol/l) solution. (C) same as B but at pH 8.30: 1, 0.02214 mmol/l TIPST and 2, TIPST (0.02214 mmol/l)–CTAB (1.00 mmol/l) micellar aggregate.

difficult in strongly acidic medium and the aggregation of too many  $\text{OH}^-$  on CTAB will occur in strongly basic medium. Because the electrostatic attraction of CTAB to  $\text{TIPST}^-$  is weaker than that of  $\text{TIPST}^{2-}$ , TIPST is easier to assemble on CTAB in a weaker basic solution than it is in a weaker acid solution. By investigating the CTAB–TIPST interaction at pH 5.89 and 8.30, curve 8 gives a lower valley than curve 12. From curve 8, the two wavelengths 630 and 590.5 nm were used in the successive experiment at pH 5.89. With the same way, both 576 and 614 nm from curve 12 were selected at pH 8.30. Figs. 2B and 2C show the absorption spectra of the TIPST solution and its CTAB aggregate without free TIPST at pH 5.89 and 8.30. The absorption peaks of TIPST are located at 595 nm at pH 5.89 from curve B-1 and 605 nm at pH 8.30 from curve C-1 and those of the TIPST–CTAB aggregate at 655 nm at pH 5.89 and 590 nm from curve C-2. The spectral red shift of the aggregate at pH 5.89 is 60 nm but the spectral blue shift of the aggregate at pH 8.30 is only 15 nm. In addition, by comparing curve 2 with 3 in Fig. 2B, the large aggregate (TIPST:CTAB = 1: $x$ ,  $x > 1$ ) shows that the spectral peak is located at 605 nm. The spectral blue shift of the large aggregate will be 50 nm against the monomer aggregate. Of course, ordinary spectrophotometry is unsuitable to the interaction of CTAB with TIPST because of very short spectral shift. The correction coefficients were calculated to be  $\beta_{\text{TIPST}} = 0.282$  at pH 5.89 from curves B-1,  $\beta_{\text{TIPST}} = 0.418$  at pH 8.30 from curve C-1,  $\alpha_{\text{CTAB-TIPST}} = 0.704$  at pH 5.89 from curves B-2, and  $\alpha_{\text{CTAB-TIPST}} = 1.03$  at pH 8.30 from curve C-2.

The effect of anionic surfactant, e.g., SDS, on the absorption spectra of the CTAB–TIPST aggregate is shown as curve B-4. Curve B-4 is coincident with curve B-1. This is attributed to the fact that SDS has replaced the TIPST binding on CTAB to form the SDS–CTAB aggregate. The replacement reaction is sensitive at pH 5.89 and it has been applied to the detection of AD in water. From curves 2 and 4, the correction coefficients  $\beta$  and  $\alpha$  are the same as the CTAB–TIPST interaction at pH 5.89.

#### 4.2. Analysis of interaction of CTAB with TIPST

It is well known that the electrolyte directly affects the CMC and the self-aggregation number of a surfactant. From the change of the surface tension of the CTAB solution as shown in Fig. 4, the CMC of CTAB drops down to 0.1 mmol/l from 0.5 mmol/l by comparing curves 2 and 3 with curve 1. It is attributed to the fact that the addition of the buffer solution has increased the electrolyte up to 0.5 mol/l. In the ammonium ( $\text{NH}_3$ ,  $\text{NH}_4^+$ ) and acetate ( $\text{HOAc}$ ,  $\text{OAc}^-$ ) medium, the hydrogen bond and electrostatic interaction of CTAB with  $\text{NH}_3$ ,  $\text{NH}_4^+$  and  $\text{OAc}^-$ ,  $\text{HOAc}$  may occur to form CTAB– $\text{NH}_3$  ( $\text{NH}_4^+$ ) and CTAB– $\text{OAc}^-$  ( $\text{HOAc}$ ) micelle complexes. Moreover, the binding number of  $\text{NH}_3$  ( $\text{NH}_4^+$ ) and  $\text{OAc}^-$  ( $\text{HOAc}$ ) will be very high because the electrolyte concentration is much more than CTAB. However, the self-aggregation of CTAB will not occur when

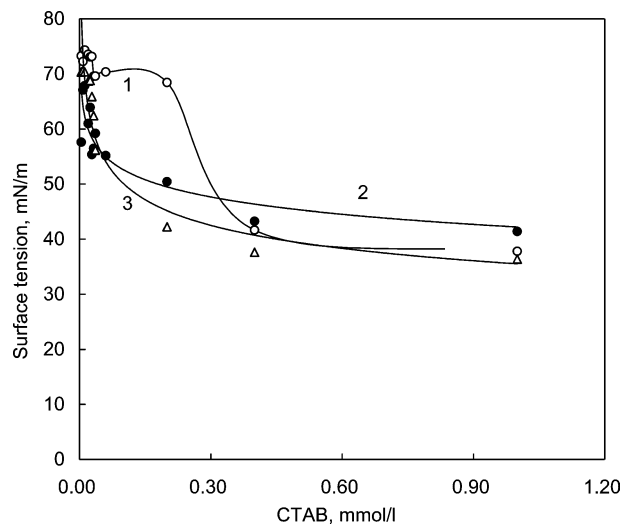


Fig. 4. (1) Change of surface tension of the CTAB solution; (2) same as 1 but in the presence of pH 5.89 buffer; and (3) same as 1 but in the presence of pH 8.30 buffer.

CTAB is below 0.1 mmol/l. Because the electrolyte–CTAB micelle complex will not cause color change of the solution, the successive experiments will not be affected.

Fig. 5 shows the effect of CTAB molar concentration on the surface tension and the absorbance ratio of the solution. From curves 2 in Figs. 5A–5F, the increase of TIPST results in a right shift of the break points. This is attributed to the fact that the TIPST substitutes  $\text{NH}_3$ ,  $\text{NH}_4^+$  and  $\text{HOAc}$ ,  $\text{OAc}^-$  of the CTAB micelle complexes. From curves 1, we can observe the right shift of the valley with increase of TIPST. Besides, the absorbance ratio rises when CTAB is over a certain concentration. This is attributed to the fact that the oppositely charged species (TIPST anions) will attract many CTAB cations to form a mixture of the CTAB–TIPST micelle complex and the CTAB self-aggregation micelle when CTAB is more than 0.1 mmol/l. In addition, we observe that the shift of breakpoint of curves 2 is always synchronous with that of curves 1. Moreover, the breakpoint of curves 2 corresponds vertically to the valley point of curve 1. This is just to indicate that both CTAB and TIPST bind each other completely only at the breakpoints, where there are no free CTAB and no free TIPST. Therefore, the valley appears at the molar ratio 1:1 of CTAB to TIPST at pH 5.89 from curves 1 and the valley at 1.5:1 of CTAB to TIPST at pH 8.30. Preliminarily, we judged the composition of the aggregates to be 1CTAB:1TIPST at pH 5.89 and 3CTAB:2TIPST at pH 8.30.

#### 4.3. Effect of ionic strength and temperature

Fig. 6 shows the influence of the electrolyte NaCl on the TIPST–CTAB aggregation at pH 5.89 and 8.30. Because the buffer electrolyte concentration has been 0.5 mol/l, the  $\text{NH}_3$  ( $\text{NH}_4^+$ ) and  $\text{OAc}^-$  ( $\text{HOAc}$ ) of the CTAB– $\text{NH}_3$  ( $\text{NH}_4^+$ ) and CTAB– $\text{OAc}^-$  ( $\text{HOAc}$ ) micelle complexes have been replaced by TIPST. This is attributed to the strong interaction

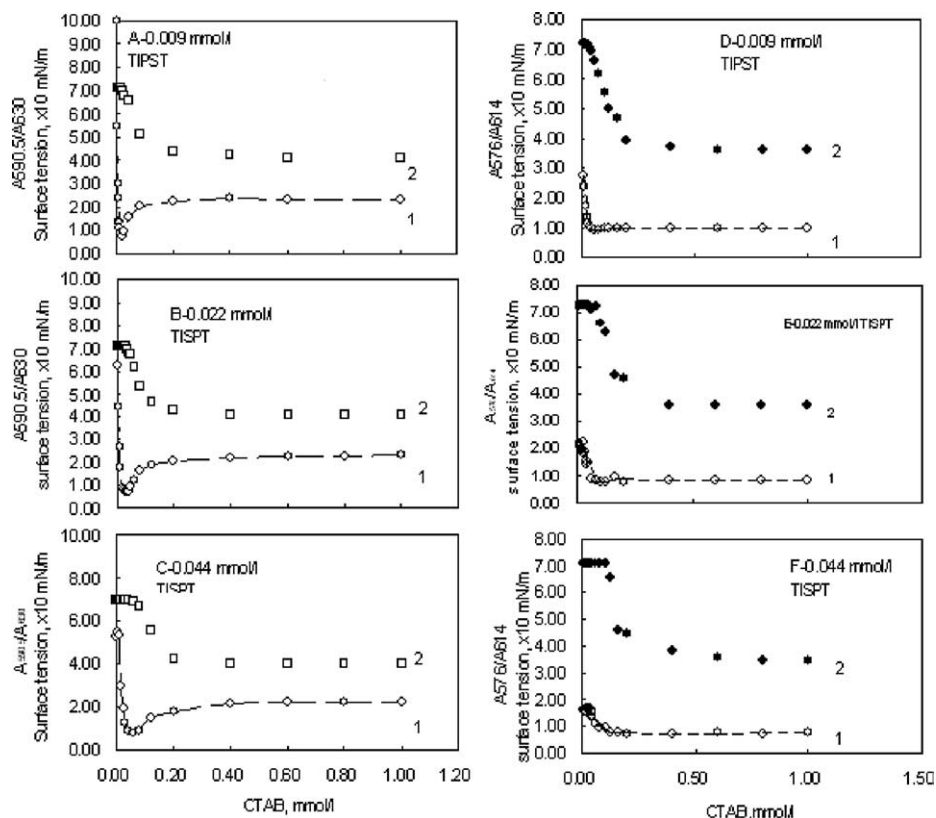


Fig. 5. (1) Dependence of  $A_{590.5}/A_{630}$  at pH 5.89 (A–C) on CTAB concentration and that of  $A_{576}/A_{614}$  at pH 8.30 (D–F). (2) Variation of the surface tension. From A to C and D to F, the solutions contained 0.009, 0.02214, and 0.04428 mmol/l TIPST, respectively.

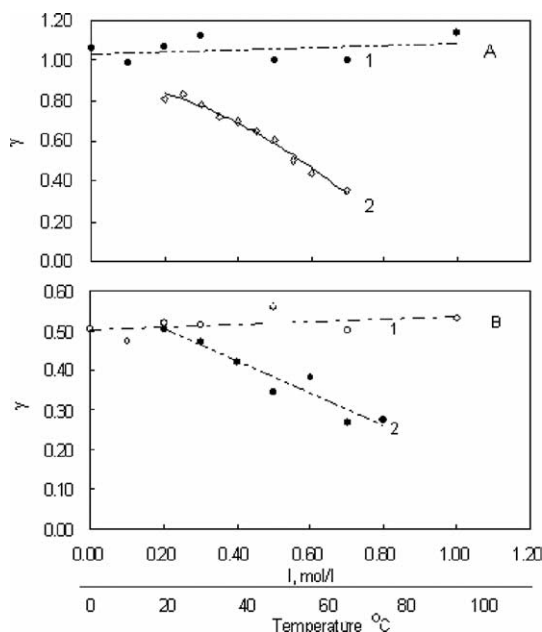


Fig. 6. Effect of ionic strength (1) and temperature (2) on  $\gamma$  of TIPST to CTAB: (A) at pH 5.89 and (B) at 8.30. All the solutions initially contain 0.008 mmol/l CTAB and 0.02214 mmol/l TIPST.

of CTAB with TIPST. Besides the electrostatic attraction, the benzene ring of CTAB will attract three benzene rings of TIPST by hydrophobic bond as polycyclic aromatic hydro-

carbons (PAH). Thus, the interaction of CTAB with TIPST is not easy for the electrolyte to destroy. Though the addition of NaCl raised the electrolyte concentration,  $\text{Cl}^-$  cannot replace TIPST of the CTAB–TIPST micelle complex. However, it can bind the free CTAB in the solution to form the CTAB–Cl micelle complex, not to cause the color change of the solution. Therefore,  $\gamma$  of TIPST to CTAB remains almost constant from curves 1. On the contrary, the influence of temperature on  $\gamma$  of TIPST to CTAB is so notable from curves 2 that  $\gamma$  decrease by 11% at pH 5.89 per increasing  $10^\circ\text{C}$  and 8% at pH 8.30. It is attributed to the fact that the noncovalent bond interaction is much weaker than any chemical bond and it is easy to destroy at high temperatures.

#### 4.4. Characterization of the CTAB–TIPST aggregation

By varying the addition of TIPST, the absorption of the CTAB–TIPST solutions at three temperatures at pH 5.89 and 8.30 was measured, where CTAB is much less than 0.1 mmol/l.  $C_L$  and  $\gamma$  of each solution were calculated and their relationship is shown in Fig. 7. All curves for  $C_L^{-1}$  vs  $\gamma^{-1}$  are linear so the aggregation of TIPST on CTAB monomer obeys the Langmuir monolayer adsorption. From the intercepts and slopes, the binding constants of the TIPST–CTAB aggregates,  $N$  and  $K$  were calculated as shown in Table 1. We have confirmed such results by

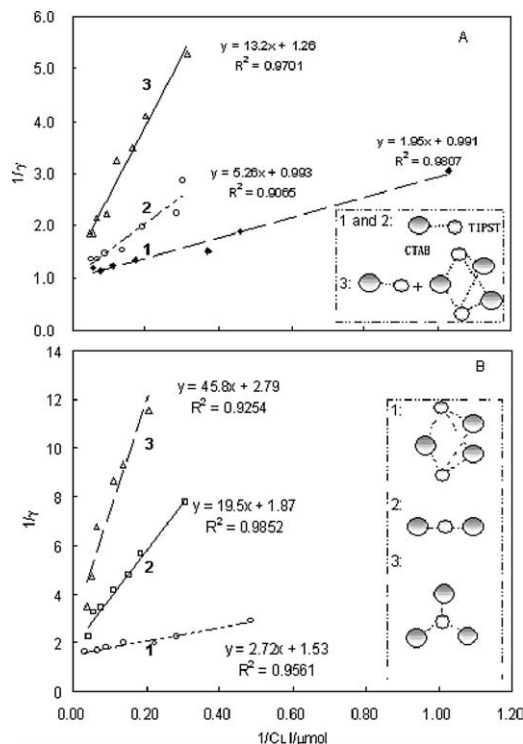


Fig. 7. Plots  $\gamma^{-1}$  vs  $C_L^{-1}$  for the interaction of CTAB with TIPST at three temperatures: (A) the solutions containing 0.0120 mmol/l CTAB and TIPST between 0.0062 and 0.031 mmol/l at pH 8.30 and (B) the solutions containing 0.0160 mmol/l CTAB and TIPST between 0.0062 and 0.031 mmol/l at pH 5.89, 1, 20, 2, 40, and 3, 60 °C.

Table 1

Determination of binding constants of the CTAB–TIPST aggregate at pH 5.89 and 8.30 at 20, 40, and 60 °C

pH of the solution	Physicochemical characterization	Temperature, °C		
		20	40	60
5.89	TIPST:CTAB ( <i>N</i> )	1:1 (1)	1:1 (1)	1:1 + 2:3 (0.75)
	$K, \times 10^5$ l/mol	5.13	1.90	0.757
	$\epsilon^{630\text{ nm}}, \times 10^4$ l mol <sup>-1</sup> cm <sup>-1</sup>	1.95	1.88	2.02
8.30	TIPST:CTAB ( <i>N</i> )	2:3 (0.67)	1:2 (0.5)	1:3 (0.33)
	$K, \times 10^5$ l/mol	5.66	0.968	0.607
	$\epsilon^{614\text{ nm}}, \times 10^3$ l mol <sup>-1</sup> cm <sup>-1</sup>	8.13	6.52	8.12

Note. *N*, binding number maximum of TIPST on CTAB monomer; *K*, binding constant of the TIPST–CTAB aggregate; and  $\epsilon^{630\text{ nm}}$ , molar absorptivity of the TIPST–CTAB aggregate at 630 nm.

other classical methods, the double phase description model [28] and continuous variations [29]. From Table 1, *K* always drops down with increased temperature and *N* becomes small at a higher temperature, such as *N* of TIPST to CTAB from 1 at 20 °C to 0.75 at 60 °C in the pH 5.89 medium and from 0.67 at 20 °C to 0.33 at 60 °C in the pH 8.30 medium and *K* from  $5.13 \times 10^5$  l/mol at 20 °C to  $0.757 \times 10^5$  l/mol at 60 °C in the pH 5.89 medium and from  $5.66 \times 10^5$  l/mol at 20 °C to  $0.607 \times 10^5$  l/mol at 60 °C in the pH 8.30 medium. Therefore, the desorption

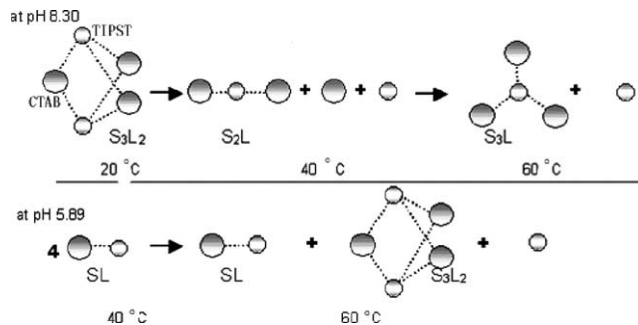


Fig. 8. Diagrammatic sketch for variation of the CTAB–TIPST aggregate with temperature.

of TIPST will occur from its CTAB aggregate when the temperature rises. The desorption process is sketched in Fig. 8. At pH 5.89, the aggregate, 1CTAB:1TIPST formed at 20 and 40 °C changes into the mixture of two aggregates: 1CTAB:1TIPST and 3CTAB:2TIPST at 60 °C. Similarly, the aggregate 3CTAB:2TIPST formed at 20 °C changes into 2CTAB:1TIPST at 40 °C and 3CTAB:1TIPST at 60 °C at pH 8.30. In addition, from Eq. (6),  $\epsilon_r^{\lambda^2}$  of the aggregate was calculated as given in Table 1. For characterization of the aggregate, the spectral correction technique is more suitable and simpler in operation than the classical methods above because of the strong light-absorption of L.

#### 4.5. Replacement of TIPST and Interaction of CTAB with SDS and SDBS

Because anionic surfactants, e.g., SDS and SDBS, have long carbon chains, they can bind CTAB to form firm micelle complexes. Besides the electrostatic attraction force, the hydrogen bond and many PAH will be formed between CTAB and SDS or SDBS. Therefore, SDS and SDBS both can replace TIPST in the CTAB–TIPST micelle complex. We found that the replacement reaction is very sensitive at pH 5.89. This is very useful to investigate the interaction of cationic surfactant with anionic surfactant and sensitive detection of anionic detergent (AD). By varying the addition of SDS or SDBS into the CTAB–TIPST complex solution,  $A_c$  of each solution,  $\eta$  of TIPST, and  $\gamma$  of CTAB to SDS or SDBS were calculated by Eqs. (7), (8), and (9). The results are shown in Fig. 9. From the regression equations, the interaction of CTAB with SDS and SDBS obeys the Langmuir isothermal adsorption in only one monolayer. The binding ratios of both SDS and SDBS to CTAB are 1.5 and the diagrammatic sketch of the aggregates is given in Fig. 9. *K* of the aggregates was calculated to be  $K_{\text{SDS-CTAB}} = 3.44 \times 10^6$  and  $K_{\text{SDBS-CTAB}} = 2.23 \times 10^6$  l/mol at room temperature. From the comparison of the slopes, SDBS has a stronger attraction force on CTAB than SDS. This is attributed to the fact that SDBS has a benzene ring to connect that of CTAB by strong hydrophobic bonding.

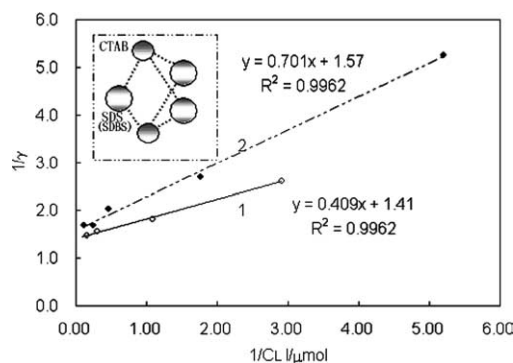


Fig. 9. Plots  $\gamma^{-1}$  vs  $C_L^{-1}$  for the interaction of CTAB with SDS at pH 5.89: (1) the solutions containing 0.020 mmol/l SDS and the CTAB-TIPST aggregate between 0.004428 and 0.0354 mmol/l and (2) the solutions containing 0.020 mmol/l SDS and the CTAB-TIPST aggregate between 0.004428 and 0.0354 mmol/l.

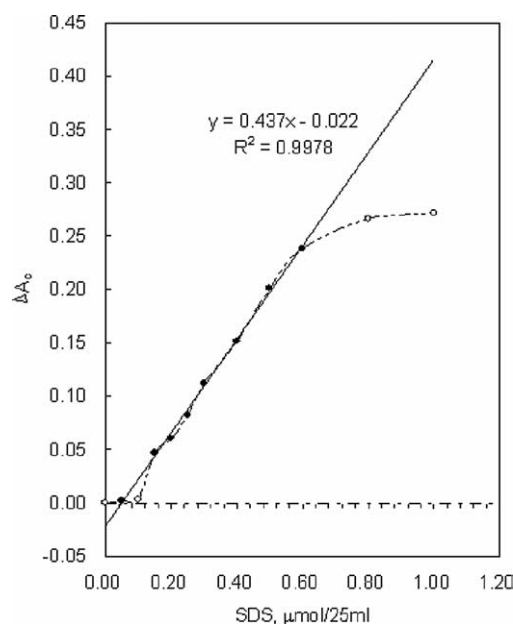


Fig. 10. Standard curve for the determination of AD with TIPST at pH 5.89 at 484.8 nm, where the solutions contain 0.0177 mmol/l CTAB-TIPST aggregate in the presence of  $\text{Na}_2\text{EDTA}$ .

#### 4.6. Application of the replacement reaction to AD detection

The standard curve,  $\Delta A_c$  vs  $x$  ( $x$  is the SDS molar number), from the series of standard SDS solutions is shown in Fig. 10 for the quantitative determination of AD in samples. We observe that it is linear between 0 and 0.600  $\mu\text{mol}$  of SDS. By adding 5%  $\text{Na}_2\text{EDTA}$  in the SDS solution, the influence of foreign substances, including ions, on the determination of CTAB was tested at pH 5.89. None affects the direct determination of 0.20  $\mu\text{mol}$  of SDS (less than 10% error): 1 mg of humic acid, amino acid,  $\text{Cl}^-$ ,  $\text{Ca(II)}$ ,  $\text{Mg(II)}$ , 0.5 mg of  $\text{F}^-$ ,  $\text{Mn(II)}$ ,  $\text{Ni(II)}$ ,  $\text{Zn(II)}$ ,  $\text{Pb(II)}$ ,  $\text{Cu(II)}$ ,  $\text{Fe(III)}$ , and  $\text{Al(III)}$ .

Table 2  
Determination of AD in water samples

Sample	To flask, added	Found, AD ( $\mu\text{mol/l}$ )
1. Lake water	10 ml of sample	$0.0213 \pm 0.0011^a$ ( $0.020^b$ ) RSD: 5.10%
	0.200 $\mu\text{mol}$ of SDS and 10 ml of sample	$0.0433 \pm 0.0006^a$ ( $0.044^b$ ) Rec. 110%
2. Huaihe river	10 ml of sample	$0.0267 \pm 0.0013^a$ ( $0.026^b$ ) RSD: 4.90%
	0.200 $\mu\text{mol}$ of SDS and 10 ml of sample	$0.0463 \pm 0.0004^a$ ( $0.047^b$ ) Rec. 97.8%
3. Local sewage	10 ml of sample	$0.0270 \pm 0.0004^a$ ( $0.027^b$ ) RSD: 1.40%
	0.200 $\mu\text{mol}$ of SDS and 10 ml of sample	$0.0476 \pm 0.0002^a$ ( $0.046^b$ ) Rec. 98.4%

<sup>a</sup> Six replicated determinations by the present method.

<sup>b</sup> Average of three replicated determinations by ISO7875-1996 [30]. RSD, relative standard deviation; Rec., recovery of SDS.

Three practical water samples were determined. Sample 1 was sampled from a lake, sample 2 from the Huaihe River, and sample 3 from a local sewage pipe. Six replicated determinations of each were made and the results are given in Table 2, the accuracy of which has been confirmed by a conventional method [30]. From Table 2, the recovery of the standard SDS added is between 97.8 and 110% with RSD less than 5.1%. Therefore, the present method is suitable for monitoring of water quality with a good selectivity.

## 5. Conclusions

Using a dye as a spectral substitute provides a novel and simple measurement approach to characterize complexation between surfactants. The cooperation of both the Langmuir isothermal adsorption and the spectral correction (MSASC) technique played an important role in the spectrometric study, which meets precision and accuracy criteria and offers the additional benefits of simplicity and versatility. We are sure that both the replacement reaction and the MSASC technique will be applied widely in the future.

## Acknowledgments

Financial support from both the National High Technology Research and Development Program of China (863 Program, No. 2002AA601320) and the National Natural Science Foundation of China (No. 50008011) is gratefully acknowledged.

## References

- [1] R.K. Dutta, S.N. Bhat, Bull. Chem. Soc. Jpn. 65 (1992) 1089.
- [2] E.W. Anacker, J. Colloid Interface Sci. 164 (1994) 54.

- [3] L.N. Gou, I. Arnaud, M. Petit-Ramel, R. Gauthier, C. Monnet, P. Le Perchec, Y. Chevalier, *J. Colloid Interface Sci.* 163 (1994) 334.
- [4] S. Bracko, J. Span, *Dyes Pigments* 50 (2001) 77.
- [5] D. Pramanick, D. Mukherjee, *J. Colloid Interface Sci.* 157 (1993) 131.
- [6] N.G. Lai, A. Isabelle, P.R. Michele, G. Robert, M. Christian, L.P. Pierre, C. Yves, *J. Colloid Interface Sci.* 163 (1994) 334.
- [7] H.J. Chen, W.G. Herkstroeter, J. Peristein, K.Y. Law, D.G. Whitten, *J. Phys. Chem.* 98 (1994) 5138.
- [8] T. Inoue, H. Ohmura, D. Murata, *J. Colloid Interface Sci.* 258 (2003) 374.
- [9] N. Lemke, J.J. Arenzon, Y. Levin, *Physica A Statist. Mech. Appl.* 300 (2001) 82.
- [10] J.T. Kunjappu, C.K.K. Nair, *Indian J. Chem. Sect. A Inorg. Bio-Inorg. Phys. Theor. Anal. Chem.* 31 (1992) 432.
- [11] V. Mrunalini, K.N.G. Pattarkine, *Biochem. Biophys. Res. Commun.* 263 (1999) 41.
- [12] M. Bergstroem, J.C. Eriksson, *Langmuir* 16 (2000) 7173.
- [13] E.F. Marques, O. Regev, A. Khan, B. Lindman, *Adv. Colloid Interface Sci.* 100 (2003) 83.
- [14] M.G. Neumann, M.H. Gehlen, *J. Colloid Interface Sci.* 135 (1990) 209.
- [15] T. Kinugasa, A. Kondo, E. Mouri, S. Ichikawa, S. Nakagawa, Y. Nishii, K. Watanabe, H. Takeuchi, *Sep. Purif. Technol.* 31 (2003) 251.
- [16] L.H. Torn, A. Keizer, L.K. Koopal, J. Lyklema, *J. Colloid Interface Sci.* 260 (2003) 1.
- [17] S.G. Cutler, P.J. Meares, D.G. Hall, *Electroanal. Chem.* 85 (1977) 145.
- [18] Y.X. Ci, M.M. Yang, *Chin. Sci. Bull.* 16 (1983) 980.
- [19] X.Y. Zheng, L.D. Li, S.Q. Sun, *Chin. J. Chem. Reagents* 6 (1994) 273.
- [20] B. Savvins, P.K. Chernova, I.L.M. Kudpatseva, *Zh. Anal. Khim.* 33 (1978) 2127.
- [21] W.B. Qi, L.Z. Zhu, *Chem. J. Chin. Univ.* 7 (1986) 407.
- [22] H.W. Gao, Q.S. Ye, W.G. Liu, *Anal. Sci.* 18 (2002) 455.
- [23] H.W. Gao, J.X. Yang, *Colloids Surf. A* 205 (2002) 283.
- [24] B. Simoncic, M. Kert, *Dyes Pigments* 54 (2002) 221.
- [25] H.W. Gao, J.F. Zhao, Z.J. Hu, *Chem. Phys. Lett.* 376 (2003) 281.
- [26] I. Langmuir, *J. Am. Chem. Soc.* 40 (1918) 1361.
- [27] H.W. Gao, P. Meng, L. Wang, *J. Ind. Chem. Soc.* 78 (2001) 9.
- [28] M. Pesavento, A. Profumo, *Talanta* 38 (1991) 1099.
- [29] W. Likussar, *Anal. Chem.* 45 (1973) 1926.
- [30] ISO, Water quality—Determination of surfactants, Part 1: Determination of anionic surfactants by measurement of the methylene blue index (MBAS), 7875 (1996).